First-principles calculation of Li adatom structures on the Mo(112) surface

A. Kiejna[1,2] and R. M. Nieminen[1]
[1]*Laboratory of Physics, Helsinki University of Technology, P.O. Box 1100, FIN-02015 HUT, Finland*
[2]*Institute of Experimental Physics, University of Wrocław, Plac M. Borna 9, PL-50-204 Wrocław, Poland*
(Received 24 April 2002; published 5 August 2002)

The formation and structure of the ordered phases of Li atoms adsorbed on the Mo(112) surface are investigated by performing first-principles density-functional calculations. Large inward relaxation for the first atomic interlayer distance of the clean Mo(112) surface is found. The vertical relaxations of the substrate are only little influenced by the adsorbed Li atoms. The magnitude of lateral shifts of atoms along the atomic rows is found to be small and in line with measured values. The energetics of chain structures of Li adatoms for coverages $0.125 \leqslant \Theta \leqslant 1$ monolayer is determined and the $p(4\times1)$ and $p(2\times1)$ adatom structures are found to be the most favored ones in agreement with experiment. The binding energy of Li atoms decreases with increasing coverage. The calculated work function changes with Li adatom coverage are in good agreement with experiment. The energy barriers for adatom diffusion are determined and the energetics of lateral interactions between adatoms is discussed.

DOI: 10.1103/PhysRevB.66.085407 PACS number(s): 68.35.Bs, 68.43.Bc, 68.43.Fg, 73.30.+y

I. INTRODUCTION

The adsorption of submonolayers of metallic atoms on metal surfaces can be strongly anisotropic. Two-dimensional structures formed by adatoms are very interesting because they provide information on the character of lateral interatomic interactions. The structure of two-dimensional adsorbate phases is determined by the potential relief of the substrate, which sets the matrix of adsorption sites, and the lateral interactions of adatoms, which decide which of these sites will be occupied. The lateral adatom interactions are usually divided into *direct* ones, due to (isotropic) repulsive dipole-dipole interactions between dipoles constituted by the adatoms and their screening charge in the substrate, and *indirect* long-range interactions via the substrate electron distribution deformed by adsorption,[1,2] which have an anisotropic character. A delicate balance between these two interactions determines the low-coverage adsorbate phases.

Close-packed surfaces or large terraces therefrom are usually considered as the ideal playground to study lateral adatom interactions. These interactions can show quasi-one-dimensional character when considering atoms adsorbed along step edges or on surfaces with strongly anisotropic relief properties. In this respect the adsorption of metallic atoms on the (112) surface of body-centered-cubic (bcc) metals is a very interesting case. This surface has a furrowed (or a two-atomic-row terrace) structure where atoms can adsorb along close-packed $[11\bar{1}]$ directions.

Adsorption of metallic atoms on the (112) surface of molybdenum and tungsten has been extensively studied experimentally, showing a diversity of ordered adatom structures with evidence for a strong anisotropy of lateral interactions. In some cases adsorbed atoms are prone to form quasi-one-dimensional chain structures.[1,3]

Particularly interesting are the commensurate chain structures of the $p(n\times1)$ type, formed by alkali and alkaline-earth metals for coverages smaller than 0.5 monolayer perpendicular to the furrows. The multiplicity factor along the rows n can vary from 2 to 4 for Li/Mo(112) and up to 8 for a Sr/Mo(112) system.[4–8] The $p(4\times1)$ and $p(2\times1)$ structures are also discovered for the Mg/Mo(112) system.[9] The adsorbed atoms in the neighboring troughs are relatively close to one another (but they do not touch each other). On the other hand, the distance between the chains is much larger and can exceed 20 Å. Apparently, for low coverages of Li and Sr, similarly as for other alkali-metal adsorbates,[10] the adatom interaction has a repulsive character. It is pronounced along the furrows but is to a large extent screened by the substrate atoms perpendicular to the furrows, making the attractive component prevailing in this direction. Interestingly, the chain structures are observed for Na but not for K and Cs on Mo(112). This suggests that relative sizes of the atoms may play a role; i.e., the repulsive interaction between adatoms is less effectively screened across the rows for the larger adatoms such as K and Cs. Thus a detailed mechanism behind the formation of these structures is not entirely clear. Simple models explaining the formation of chains based on theoretical calculations[11] and lattice-gas model simulations[12] suggest that what is responsible for the formation of the observed structures is the dipole-dipole interactions mediated by the local distortion in the substrate electron distribution due to the adsorbed atom. This distortion is screened by Friedel oscillations of the electron distribution and leads to an oscillatory interaction potential of long-range character. The minima in the potential have a periodicity of twice the Fermi wave number and thus depend on the substrate band structure. The validity of these models is, however, limited to relatively low coverages. On the other hand, the structural complexity of furrowed surfaces requires large supercells to treat, which makes them difficult to access by first-principles methods.

In this work we present results of extensive first-principles calculations for different chain structures formed by Li atoms on Mo(112). Our results provide information on the geometry and stability of the formed structures, on the energetics of structural phase transitions occurring in the adsorbed layers when the adatom coverage varies, and on the

character of adatom interactions. We also calculate the energy barriers for Li diffusion along the furrows. We concentrate on the ordered phases of the Li adlayers corresponding to coverages of up to one monolayer (ML). The first-principles calculations demonstrate that Li(4×1)- and Li(2×1)-ordered structures observed experimentally on the Mo(112) surface at coverages 0.25 ML and 0.5 ML, respectively, are energetically more stable than any other configurations.

II. METHODS OF CALCULATION

The calculations presented in this work employ density-functional theory[13,14] (DFT) in the generalized gradient approximation (GGA) for the exchange-correlation energy functional,[15] ultrasoft pseudopotentials[16] to represent the ionic cores, and the plane-wave basis set as implemented in the VASP code.[17] The basis set includes plane waves with energy up to 250 eV. The clean Mo(112) surface is modeled by periodic slabs consisting of seven molybdenum layers (9 Å thick) separated by eight equivalent layers (10.3 Å) of vacuum. The Li atoms are adsorbed on one side of the slab and the electric field arising due to the asymmetry of the system is compensated for by a dipole correction.[10] The positions of atoms in the four topmost molybdenum layers and of all the adsorbed atoms are optimized by requiring that the forces on all unconstrained atoms converge to less than 0.025 eV/Å. The equivalent mesh $20\times12\times1$ of up to 60 Monkhorst-Pack[18] special **k** points to sample an irreducible segment of the $1\times1\times(7+8)$ orthorhombic unit cell (and proportionally reduced depending on the size of supercell) and a Methfessel-Paxton method[19] with a smearing of 0.2 eV are applied to Brillouin-zone integrations.

The calculations have been performed for Li coverages $1/8\leqslant\Theta\leqslant1$ and different sites above the top Mo layer. The coverage Θ is defined as the ratio of the number of adsorbed atoms to the number of atoms in an ideal substrate surface unit cell. The stability of Li adatom structures is considered by analyzing the adatoms energetics. The binding energy per adatom for a given Li coverage is calculated as the average energy difference

$$E_b(\Theta)=-\frac{1}{N}(E_{\mathrm{Li/Mo(112)}}-E_{\mathrm{Mo(112)}}-NE_{\mathrm{Li}}), \qquad (1)$$

where N is the number of Li atoms per unit cell and $E_{\mathrm{Li/Mo(112)}}$ is the total energy of the Mo(112) slab with adsorbed Li atoms, while $E_{\mathrm{Mo(112)}}$ and E_{Li} represent the total energies of the relaxed Mo(112) surface and the isolated Li atom, respectively.

III. RESULTS AND DISCUSSION

A. Clean Mo(112) surface

Before studying the effect of Li adsorption on the Mo(112) surface, we first determine the bulk and bare-metal-surface structure. The calculated GGA lattice constant of bcc Mo is 3.152 Å which agrees very well with the experimental value 3.15 Å.[20] The bulk modulus of 2.52 Mbar is in between two measured values 2.3 Mbar (Ref. 21) and 2.73 Mbar (Ref. 20), 8% lower than the maximum of the two values. The first-principles calculations of Ref. 22 performed within the local density approximation (LDA) gave, respectively, 3.16 Å for the lattice constant and 2.8 Mbar for the bulk modulus.

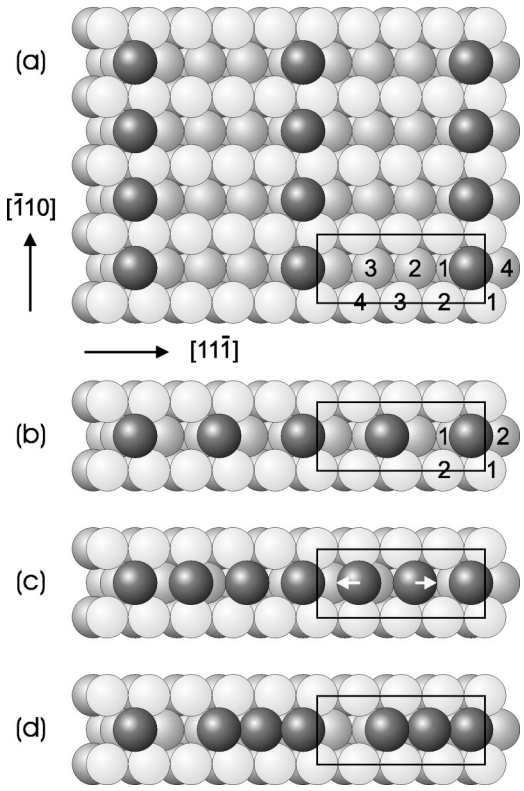

FIG. 1. Top view of different Li structures (dark balls) on the Mo(112). (a) The $p(4\times1)$ and (b) $p(2\times1)$ chain structures. The numbers on the Mo atoms of the first and second rows are used to label atomic shifts in Table IV. Two possibilities for incommensurate structures for $\Theta=3/4$ coverage are shown in (c) and (d). The arrows indicate the direction of calculated shifts of the adatoms (see discussion for high-coverage structures).

Figure 1 illustrates the atomic structure of the (112) surface of a bcc crystal. Clean Mo(112) has recently been studied both theoretically[22] and experimentally.[23] The calculations reported here for a 1×1 surface unit cell, while in general agreement with these earlier results, show, however, some differences. The calculated relaxations $\Delta_{ij}=(d_{ij}-d_0)/d_0$ of interlayer spacing between layers i and j with respect to the spacing $d_0=1.29$ Å between bulk planes are presented in Table I for the four topmost atomic layers of the Mo(112). The Mo atoms have also freedom to relax along the $[\bar{1}11]$ direction—i.e., along the furrows. The respective displacements are also shown in Table I. As already mentioned, the furrowed (112) surface is an example of a vicinal surface with two atom rows on each terrace. According to the general model based on the Smoluchowski smoothing effect[24,25] and experimental findings[26] of the l rows of atoms on each terrace, the first $l-1$ (i.e., in our case one) exhibit contraction, while the final lth row relaxes outward (expands). Our results show a 17% contraction of the interplanar distance for the topmost atomic plane, in agreement with

TABLE I. Structural parameters for the four uppermost layers on clean Mo(112). Δd_{ij} are the vertical relaxations of interlayer distance (in % of the bulk interlayer spacing). x_i is the lateral displacement (in Å) of the Mo atoms of a particular layer in the direction along the rows.

Δd_{12}	Δd_{23}	Δd_{34}	Δd_{45}	Reference
-17.7	-1.2	2.9	-0.36	This work (GGA)
-16.2	2.9	-1.9	2.2	LDA[a]
-16 ± 2	2 ± 3	-2 ± 3	0 ± 4	Expt.[b]
x_1	x_2	x_3	x_4	
0.04	0.01	-0.07	-0.03	This work (GGA)
0.02	0.04	-0.04	-0.01	LDA[a]
0.10	0.05	-0.03	0.02	Expt.[b]

[a]Reference 22.
[b]Reference 23.

both recent first-principles calculations[22] and experimental values[23] (as well as with the Smoluchowski model[24,25]). Relaxation of deeper layers is relatively small. However, the multilayer relaxation pattern obtained by us as a function of increasing depth from the surface of the form $--+-$ disagrees with a $-+-+$ sequence that was determined in another DFT calculation[22] and experiment.[23] Here the minus and plus signs denote contraction and expansion, respectively. One reason for this difference might be the use of different exchange-correlation functionals in our calculation (GGA instead of LDA). On the other hand, the multilayer relaxation sequence calculated by us is consistent with that calculated for another transition metal, tungsten, in Ref. 27 using the point ion model and truncated bulk electron density. To clarify if this discrepancy could originate from a thinner slab used by us, we have performed calculations for a thicker slab of 11 atomic layers, with 7 layers allowed to relax. This resulted in the following relaxation of the subsequent layers: $\Delta_{12}=-18.7\%$, $\Delta_{23}=0.97\%$, $\Delta_{34}=-0.22\%$, $\Delta_{45}=3.1\%$, and $\Delta_{56}=-1.5\%$. These numbers give a correct relaxation pattern $-+--+$ but the magnitude of Δ_{12} is in less satisfactory agreement with experiment than for the former calculation. For our further study of adsorption the most important issue is the first interlayer distance, which for a 7-layer slab agrees both with experiment and other calculations. Therefore, we conclude that a 7-layer slab is thick enough to give reliable structure for the Mo(112).

This is confirmed by results for the other important surface characteristics of electronic origin: the surface energy and the work function. The surface energy calculated in this work within GGA is 2.38 eV/atom and coincides with the value reported in Ref. 22 for the LDA calculations. The calculated work function is 4.25 eV for the relaxed 1×1 surface unit cell and 4.35 eV for the $2\times2\times(7+8)$ supercell. These values agree very well with the work function measured by photoemission, equal to 4.36 eV.[28]

B. Structures of Li adatoms on the Mo(112)

The determined surface structure of the clean Mo(112) is used as a reference system for the calculation of the structure and energetics of adsorbed Li submonolayers for coverages $1/8\leqslant\Theta\leqslant1$. In order to limit the number of possible atomic configurations, guided by experiment,[5] we have assumed that the most favored adsorption sites for Li atoms are given by the bulk (volume) site geometry. This corresponds to the position that would be occupied by atoms of an additional substrate layer. It means that for one monolayer coverage ($\Theta=1$) the Li adatoms in a starting geometry form a pseudomorphic layer. Some of the considered Li coverages require the initial position of the second or third adatom in the bridge or hollow site. These, however, appeared unstable and the atoms were shifted towards volume positions. Long-range lateral interactions that lead to the formation of the low-coverage (chain) phases of the $p(n\times1)$ type with $n\leqslant8$ require relatively large surface unit cells. The adsorption of Li atoms on the Mo(112) induces changes to the surface structure and the electronic properties which are discussed below.

TABLE II. Binding energies of Li atoms on Mo(112) for different coverages and dimensions of surface unit cells used in the calculations. For the values marked by an asterisk the forces on the atoms have converged to less than 0.03 eV/Å (instead of 0.025 eV/Å). The position of a single Li atom in a volume site is denoted by A. The neighboring volume sites are denoted by B,C,D, . . . , respectively. The corresponding sites in a subsequent furrow are labeled by lower case letters, respectively.

Coverage (ML)	Surface cell	Li atom positions	E_b (eV)
1/8	8×1	A	2.881
	4×2	A	2.844
1/4	4×1	A	2.881
	8×1	AB	2.862
	8×1	AC	2.867
	8×1	AD	2.870*
	8×1	AE	2.875*
	2×2	A	2.823
	4×2	AB	2.811
	4×2	AC	2.831
	4×2	Aa	2.880
	4×2	Ab	2.851
	4×2	Ac	2.818
1/3	3×1	A	2.875
1/2	4×1	AB	2.859
	4×1	AC	2.853*
	8×1	ACEG	2.850
	2×2	AB	2.716
	2×2	Ab	2.846
2/3	3×1	AB	2.848
3/4	4×1	ABC	2.836
1	1×1	A	2.792
	3×1	ABC	2.788
	4×1	ABCD	2.785

In Table II we have collected the binding energies with respect to the energy of a free Li atom, calculated for different coverages and a variety of surface unit cells considered in this work. These include the 4×1, 4×2, 8×1, 3×1, and

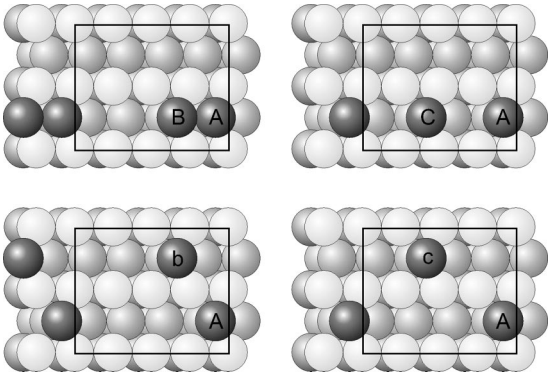

FIG. 2. Geometry of two Li adatoms on the Mo(112) surface for the (4×2) cell. A second Li atom is adsorbed at the bulk sites along the atomic furrows, at different distances from the initial Li atom. The configurations of Li atoms in the unit cell are denoted as AB, AC, Ab, and Ac. The labeling corresponds to that adopted in Table II.

2×2 cells. Some of them are illustrated in Figs. 1–3 (see also Fig. 8). Inspection of binding energies of Li atoms in different surface unit cells shows a tendency to the preference of linear (chain) structures across the rows over the clustering or formation of linear structures along the rows. Also the more homogeneous distribution of Li atoms, such as the $c(4\times2)$ structures (A-c structure in Fig. 2), are less favored. The differences in the binding energy usually amount up to several tens of meV. For the most strongly bound atom for the (4×1) structure and the most weakly bound atoms in the 2×2 unit cell, this difference is 165 meV. On the other hand, the error bars for the calculated binding energies, due to different sizes of unit cells and different number of **k** points applied, which could be estimated by comparing the numbers for a single Li atom in the 4×1 and two evenly spaced Li atoms in 8×1 cell (Figs. 1 and 3), amount to about 6 meV. Calculations for the (4×1) structure of 2 Li atoms in the 8×1 and 4×2 cells (with $2\times12\times1$ and $5\times6\times1$ **k**-point meshes, respectively) give the E_b's which agree to within 5 meV. A similar comparison of the binding energies for a monolayer coverage of Li calculated for the 1×1, 3×1, and 4×1 unit cells gives differences within 7 meV. Thus one can accept ±5 meV as the accuracy in the determination of the relative energies in different unit cells.

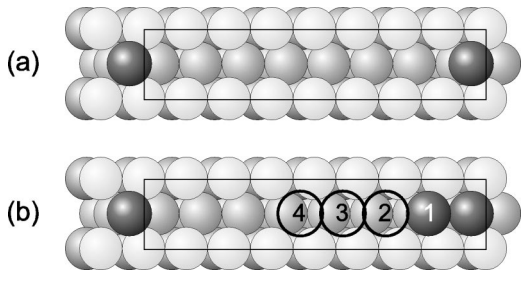

FIG. 3. (a) The positions of a single Li atom in the 8×1 surface cell. (b) The positions of a second Li atom adsorbed at the subsequent bulk sites, at different distance from the initial Li atom, along the atomic furrows. The numbers show the multiplicity of surface lattice parameter.

TABLE III. Binding energies of Li atoms adsorbed on Mo(112) for different coverages and surface unit cells. d_{Li} is the average distance of a Li adatom to the topmost Mo layer. ΔE_b is the difference in binding energies E_b per Li adatom with respect to the binding for the coverage $\Theta=1/8$ ML.

Coverage (ML)	Surface cell	d_{Li} (Å)	E_b (eV)	ΔE_b (eV)
1/8	8×1	1.61	2.881	0.000
1/4	4×1	1.61	2.881	0.000
1/3	3×1	1.60	2.875	−0.006
1/2	4×1	1.59	2.853	−0.028
2/3	3×1	1.56	2.848	−0.033
3/4	4×1	1.55	2.836	−0.044
1	1×1	1.48	2.792	−0.089

It is interesting to compare (Table II) the binding energy of the second Li atom calculated for the coverage $\Theta=0.25$ but in two different surface unit cells: 8×1 presented in Fig. 3 and 4×2 cell (Fig. 2). The letter A denotes the initial position of a single Li atom, and B, C, D, . . . , denote the nearest-neighbor and subsequent volume position of a second Li adatom along the same row. The corresponding Li positions in a neighboring row presented in Fig. 2 are labeled by a lowercase letter (b and c). The formation of the (4×1) chain structures across the rows is favored over clustering along the rows and over the scattered structures which are represented in Fig. 2 by different structures for a 4×2 cell. If the positions of atoms of the neighboring furrows are initially shifted from the straight chain structure A-a (not shown), sitting in the neighboring sites (a zigzag chain A-b in Fig. 2), the forces acting along the atomic furrows tend to align the atoms in the direction perpendicular to the furrows. It is seen (Table II) that for a 4×2 cell the presence of Li adatoms in a neighboring furrow increases the bonding of Li adatoms and the stability of structures is increasing with aligning adatoms normal to the furrows.

Table III shows selected binding energies of Li atoms adsorbed at the Mo(112) for most favored structures at a given coverage and different surface unit cells. It is clearly seen that the binding energy decreases with increasing coverage. The changes in the binding energies are small, however, and vary between 6 meV, for $\Theta=1/3$, and 90 meV for full monolayer coverage. Interestingly, the decrease in the binding energy with coverage is accompanied by a small but systematic decrease in the vertical distance of the Li adatom to the underlying Mo plane: $d_{Li}=1.61$ Å for a 1/4 ML and 1.47 Å for 1 ML of Li. Note, however, that in the range of small coverages $1/8\leqslant\Theta\leqslant1/2$ this decrease amounts only 0.02 Å. This decrease of the vertical bond length does not occur at the expense of the coordination as happens during alkali-atom adsorption for some other systems.[29] For all considered structures Li adatoms tend to occupy the fivefold-coordinated volume positions and the calculated shifts from these sites are small and rather increase this coordination.

The contraction of the interlayer distance between the topmost Mo layers decreases with increasing Li coverage on the surface, from −17.7% for a clean surface down to −14.7% for full monolayer coverage. It also implies a simi-

TABLE IV. Changes in the geometry (in Å) of the Li $p(2\times1)$ and $p(4\times1)$ structures on Mo(112). d_{ij} is the interlayer distance, x_{ij} are the lateral displacements of the jth atom in the ith layer, and z_{ij} are the vertical shifts of the atoms of the ith plane relative to its center-of-mass position. The numbering of atoms in the first and second atomic rows refers to the labels shown in Figs. 1(a) and 1(b). The bulk interlayer spacing $d_0=1.29$ Å.

Layer separation			Lateral shift			Vertical shift		
	Theory	Expt.[a]		Theory	Expt.[a]		Theory	Expt.[a]
				Li(2×1)				
d_{Li}	1.59	1.64	x_{Li}	−0.12	−0.14			
d_{12}	1.07	1.09	x_{11}	−0.04	−0.07	z_{11}	−0.03	−0.01
			x_{12}	−0.03	−0.08	z_{12}	0.03	0.01
d_{23}	1.29	1.34	x_{21}	−0.04	0.02	z_{21}	0.001	−0.01
			x_{22}	−0.02	0.03	z_{22}	−0.001	0.01
				Li(4×1)				
d_{Li}	1.61	1.65	x_{Li}	−0.09	−0.33			
d_{12}	1.07	1.08	x_{11}	−0.06	−0.05	z_{11}	−0.02	0.04
			x_{12}	0.01	−0.01	z_{12}	0.03	−0.03
			x_{13}	−0.01	−0.06	z_{13}	−0.01	−0.00
			x_{14}	−0.09	−0.15	z_{14}	+0.00	−0.01
d_{23}	1.28	1.37	x_{21}	−0.04	−0.07	z_{21}	0.00	0.02
			x_{22}	−0.02	0.01	z_{22}	−0.00	−0.00
			x_{23}	−0.02	−0.06	z_{23}	0.00	0.01
			x_{24}	−0.01	−0.04	z_{24}	0.00	−0.03

[a]Reference 5.

lar change in the relaxations of the deeper Mo layers. On the other hand, the vertical shifts of the atoms of the particular planes relative to the center-of-mass position (surface rumpling) are small and do not exceed 0.04 Å for all considered structures. The changes in the Mo(112) geometry for the Li(2×1) and Li(4×1) structures are presented in Table IV.

Figure 4 displays the work function variation due to Li atoms adsorbed in the most favored structures for a given coverage (compare with Table II). The scattering of the data due to different adlayer structures is rather small. The work function versus coverage curve shows a variation typical for alkali metal adsorption.[30] After initial (linear) decrease for $\Theta\leqslant0.25$, it reaches a minimum close to the 0.5 ML coverage, which indicates the transition towards less ionic and more metallic bonding. The work function lowering $\Delta\Phi$ for $0\leqslant\Theta\leqslant0.5$ amounts to about 1.2 eV and is smaller than the measured decrease of 1.45 eV.[5] Moreover, the experimental $\Delta\Phi(\Theta)$ curve does not show a minimum close to $\Theta=0.5$ but only an inflection point around 0.6–0.7 ML coverage. It is worth noting that such a shape of the work function change curve is measured for Sr/Mo(112) system.[6] On the other hand, the slope of the experimental and theoretical curves for $\Theta\leqslant0.25$, which could be taken as a measure of the initial dipole moment, agree to within 5%, thus demonstrating the agreement of the measured and calculated dipole moments (1.4 D). All these facts seem to support the view that the classical Langmuir-Gurney picture[29] of alkali-metal adsorption is also valid for the Li/Mo(112) system.

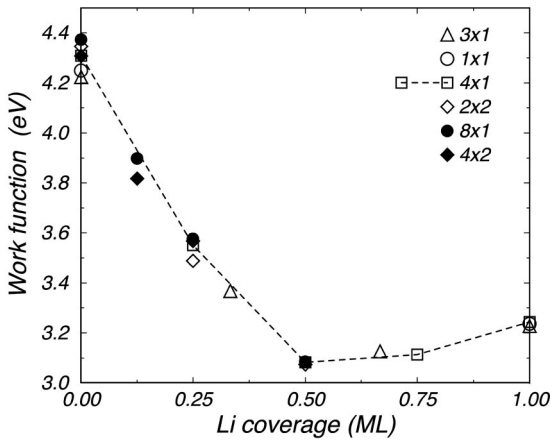

FIG. 4. Work function changes induced by Li adatoms on the Mo(112) surface. For each coverage only the work function values of the most stable structures (calculated in different surface unit cells) are plotted.

C. Low-coverage ($\Theta\leqslant0.5$) structures of Li/Mo(112)

An inspection of the binding energies of Li adatoms in different structures formed at Mo(112) shows that chain structures of different periodicity in the direction perpendicular to the furrows are energetically favored.

Experimentally one observes[4,7] stable (4×1) and (2×1) Li structures in this range of coverages. First, faint spots of the $p(4\times1)$ phase appear already at a coverage $\Theta=0.1$.[7] Our calculation shows a stable $p(8\times1)$ structure at $\Theta=0.125$, which is characterized by the same binding as the $p(4\times1)$ structure for $\Theta=1/4$. The (8×1) pattern is not observed experimentally. Because the Li(4×2) structure is almost 40 meV less stable, our results suggest that even at these low coverages (when the Li adatoms occupy to a large extent random positions) the repulsive interaction is effective along the furrows while perpendicular to them Li adatoms show a tendency towards formation of chains.

In Table IV, the data on the lateral and vertical relaxations of the adatom and the atoms of the two topmost Mo layers are compared with the results obtained from the low-energy electron diffraction (LEED) analysis.[5] The agreement is good for the geometric position of the Li adatom and the positions of the topmost layers, especially for the Li(2×1) structure. For the Li(4×1) the Li atom is less shifted than suggested by experiment. As expected, the shifts of atoms of the second and third (not shown) Mo layers are of comparable size but differ in phase. A reason for this discrepancy is the different relaxation pattern of the substrate atomic layers discussed above (Sec. III A).

Figure 5 shows the calculated bond lengths between Li and Mo atoms and compares them with measured values.[5] The agreement with experiment is within 0.05 Å for the binding of Li to Mo atom of the second Mo layer. In contrast to experiment we obtain nearly constant or slightly decreased bond lengths as the coverage is increased. This disagrees with the classical Langmuir-Gurney model[29] which predicts an increased alkali-atom bond length for a higher coverage. A rapid decrease of the work function which occurs for

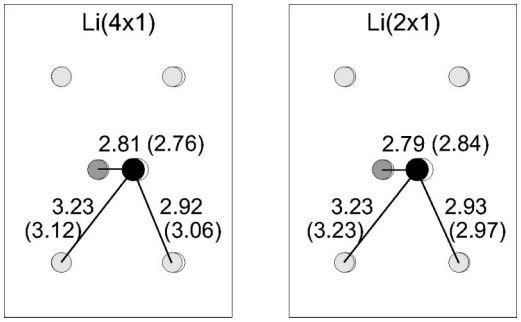

FIG. 5. Bond lengths (in Å) for the final geometry of the Li(2 $\times$1) and Li(4$\times$1) structures on Mo(112). The black circle represents the position of a Li atom. The dark-grey circle in the middle represent Mo atoms of the second atomic plane. The initial positions of atoms are shown by white (underlying) circles. The numbers in braces represent measured values.

$0.25 \leqslant \Theta \leqslant 0.5$ indicates a large charge redistribution with increased coverage. This change in the electron density distribution has almost no influence in the chemisorption bond length. On the other hand, the values for the bond length are close to the sum of metallic radii for Li-Mo which gives 2.96 Å,[20] pointing to a strong metallic contribution to the bond. This also has an impact on the most favored Li sites which appear to be the volume sites. Similarly as in experiment[5] we find that the Li sites are shifted from the ideal site of atom of the next substrate layer, although the calculated shifts are smaller. Adsorbing a second Li atom on the Li(8$\times$1)/Mo(112) surface in consecutive sites along the furrows (Fig. 3) shows that the binding attains maximum for the Li(4$\times$1)/Mo(112) structure—i.e., having Li atoms in A and E positions (Table II). The effect is quite subtle, however, because the differences in the binding in particular sites are of the order of several meV.

A strong anisotropy of the surface will be also reflected in the variation of the diffusion parameters. At not too high temperatures the diffusion across the furrows is prohibited and it will have one-dimensional character along the furrows.[31] Figure 6 displays the calculated energy barriers

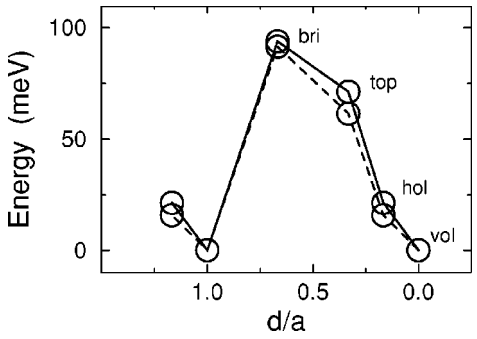

FIG. 6. The total energy difference for a single Li atom at different points along the diffusion path in the $[11\bar{1}]$ direction calculated in the 8$\times$1 and 4$\times$2 unit cells (dashed and solid lines, respectively). The labels denote volume (vol), hollow (hol), atop of Mo atom (top), and bridge (bri) sites. The distance is measured in units of surface lattice parameter $a=2.73$ Å.

for a Li atom moving along the furrow between two volume sites in 8$\times$1 and 4$\times$2 unit cells. They were calculated as the total energy difference between adatom placed in a given site and in a (stable) volume site. The barriers are below 95 meV and their magnitude compares well with the measured barriers for diffusion[31] in this system. A small difference in the energy (5–10 meV) for two different unit cells shows the effect of proximity of adatoms in the neighboring furrows. The coupling along the chains weakens the binding to the substrate and leads to a slightly lower barrier for a diffusion along the furrows. Diffusion across the atomic rows via a pass between two Mo atoms requires energy an order of magnitude larger than for diffusion along the rows. The energy barrier for crossing the trough-row system is 0.75 eV for a 4$\times$2 cell and 0.86 eV for a 8$\times$1 cell (the latter case corresponds to a proximity of Li atoms in neighboring furrows).

As already mentioned in Sec. I, the long-distance ordering of Li atoms is connected with the oscillatory character of electron screening. The Friedel oscillations of the electron distribution involve Shockley-type surface states band to be effective.[32] These interactions decay with adatom separation d, as $\sin(2k_F d)/d^2$, where k_F is the Fermi wave vector. The results of a band structure calculation for the clean Mo(112) surface[33] show that surface resonances give the main contribution to the density of states at the Fermi level. The observed crossing of the Fermi level by a surface resonance band, when moving away from the center of the zone, shows that they contribute to the development of the chain structures. The calculated band structure has been confirmed by recent measurements.[34] Another contribution to adatom interactions comes from elastic interactions due to atomic relaxations in the adsorbate/substrate system. This interaction falls of asymptotically as $1/d^3$ (Ref. 35).

In order to check a possibility of exploiting this system to study the unidirectional adatom interactions at the surface we have performed additional calculations for two adatoms interacting in a 8$\times$1 unit cell. One Li atom is adsorbed in a volume site at the edge of a long surface unit cell and the other atom is placed at consecutive on-top, bridge, and volume sites along the furrow (Fig. 3), distant by $a/3$, $2a/3$, and a from the original volume site (a is surface lattice parameter). In the calculations for on-top and bridge positions the adatom coordinate parallel to the groove was fixed. Figure 7 displays the adsorbate-adsorbate binding energy

$$E_{aa}=E_2+E_0-2E_1, \tag{2}$$

which is defined[36] with respect to the energy of two isolated adatoms. The subscripts correspond to the number of adatoms in the supercell. As is seen (Fig. 7) the stronger binding is for a second adatom placed in volume sites (integer d/a). It is also seen that the strongest binding is for the $d/a=4$—i.e., for the (4$\times$1) structure. On the other hand, the supercell is apparently too small to observe the asymptotic long-range periodicity of the interaction. Some part of this interaction, which originates from the elastic interaction, could be discriminated and quantified by performing similar calculations for a frozen surface.[36] However,

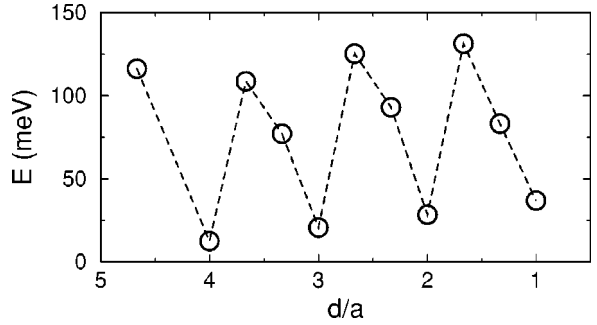

FIG. 7. The binding energy $E_{aa}=E_2+E_0-2E_1$ between two Li adatoms on the Mo(112) surface as a function adatom separation d. The subscripts denote the number of Li adatoms in the surface unit cell. One atom is placed in a preferred volume site and a second one is placed at different sites along the furrow ($[11\bar{1}]$ direction). The distance is measured in units of surface lattice parameter, $a=2.73$ Å, and the positions of succesive volume sites correspond to the numbers shown in Fig. 3. The maximum adatom separation is ~ 11 Å (half the length of the unit cell).

judging from a small influence of the adsorbate on the substrate geometry we suspect that this contribution is small and therefore it was not considered here. We should also note that the binding energies shown in Fig. 7 are calculated in a narrow cell and thus are influenced by the adatoms from the neighboring grooves. However, as already mentioned above, the proximity of adatoms from neighboring furrows lowers the binding energy only by about 5%–10%. The energies displayed in Fig. 7 provide also information on the effect of indirect interaction on the adatom diffusion. As can be seen (by comparing Figs. 6 and 7) the interaction of adatoms along the furrows increases the energy barrier by about 20 meV. The latter is comparable to the size of fluctuations in activation energy for self-diffusion at close packed (111) surface of Al and Cu.[36]

D. High-coverage ($0.5<\Theta\leq 1$) structures of Li/Mo(112)

For coverages $\Theta>0.5$, experiment[7] suggests the appearance of stable incommensurate Li structures. Close to $\Theta=2/3$ a $p(1.5\times 1)$ structure (Fig. 8) is found.[7] Our calculations show that this structure is relatively stable (Table III) although the magnitude of the adsorbate-substrate potential modifies slightly the equidistant spacing between adatoms. A finite temperature ($T>100$ K) maintained during experiment may slightly activate Li adatoms, thus allowing them to keep uniform spacing in a row. At a further increase of the coverage, around $\Theta=0.75$, an incommensurate structure with an oblique unit cell of adsorbates appears. In this structure, discovered by experiment,[7] the Li adatoms located equidistantly in each furrow are shifted rigidly in the neighboring furrow to form chains in the direction which is tilted by a small angle to a normal to the furrows. This finding was interpreted as evidence for a Li-concentration-driven second-order transition between rectangular and oblique structures.[7] The latter structure requires too large a unit cell to be treated by our calculations. Instead we have checked the stability of the incommensurate structure corresponding to $\Theta=3/4$ [Figs. 1(c)–1(d)]. Interestingly, the Li atoms which are evenly distributed along the furrow [Fig. 1(c)] do not remain pinned in their initial positions but are shifted to form three-atom chains along the furrows (as indicated by the arrows). Thus, starting the calculation for a structure with Li atoms in volume ABC sites and another one with one Li atom in the bridge position, one atop (above the atom of the second Mo layer) and one in a volume position end up with the same ABC structure [Fig. 1(d)]. Apparently, the bridge and on-top sites are strongly unfavored. This indicates a weakening of the coupling in the original chain directions and a dominating role of interactions along the furrows. It also seems to exclude the possibility for the transformation of the rectangular structure to an oblique one which is suggested[7] to occur at coverage $\Theta=3/4$. However, it is a zero-temperature calculation and the above-mentioned phases are observed at finite temperatures. Moreover, the skew angle of the structure varies (weakly) with temperature,[7] so it was suggested that at high coverages the adsorbate layer forms a floating solid. The nature of lateral interactions is also changed compared to low coverages and they are dominated by direct repulsion between the adatoms. The bonds across the furrows are weakened and the complete rows of Li atoms in the individual furrows can be shifted against each other. This shift can be explained by a phenomenological, coverage-driven mechanism of the decrease of the shear modulus in the adsorbed layer.[7] Our results show that this scenario is plausible. The adatoms of the $\Theta=2/3$ phase are by 45 meV weaker bound than those of the (4×1) phase (Table II). It means that the barrier for their activation is reduced by one-half. Thus, at room temperature they almost do not see any barrier and can easily form floating rows of evenly spaced atoms.

At monolayer Li coverage a commensurate $p(1\times 1)$ adlayer structure is observed.[4] It should be noted that due to the nearly similar sizes of Li and Mo atoms the substrate atoms are not completely screened by Li. Our calculation shows that the atoms of this pseudomorphic adlayer are by 80 meV more weakly bound than those of the $p(4\times 1)$ phase.

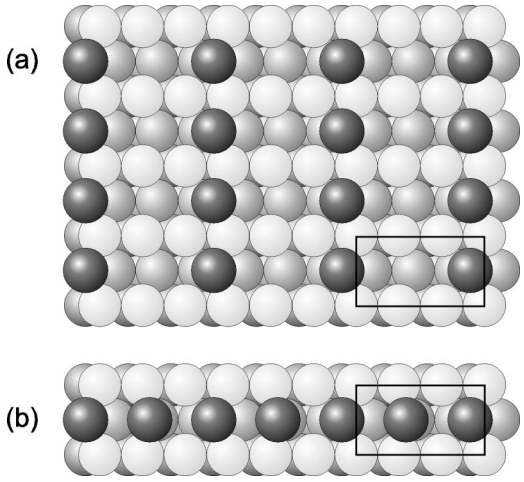

FIG. 8. Top views of the $p(3\times 1)$ and $p(1.5\times 1)$ structures formed by Li adatoms on the Mo(112).

IV. SUMMARY

We have presented results of the extensive calculations of the equilibrium atomic structure of the relaxed clean Mo(112) surface and different two-dimensional structures formed by adsorbed Li atoms for coverages $1/8 \leqslant \Theta \leqslant 1$. A very large ($\sim 17\%$) inward relaxation of the topmost Mo layer is confirmed for clean Mo(112). For a higher Li coverage the contraction of the topmost layer is reduced. The energetics of chain structures of Li adatoms is determined, and good agreement with experiment is found. The binding energy of Li atoms decreases with increasing coverage. Our calculations show that $p(4\times1)$ and $p(2\times1)$ are the most stable Li structures in the range of coverages considered. The possibility of stable Li(8×1) structures at very low coverages is suggested. The work function changes for Li adatom coverages $1/8 \leqslant \Theta \leqslant 1$ are calculated, and good agreement with experiment is found. The work function variation with coverage is consistent with the classical Langmuir-Gurney picture of alkali-metal adsorption. The energy barriers for Li atoms diffusion along the furrows are an order of magnitude lower than those for a diffusion across the furrows are, thus confirming the unidirectional character of diffusion on this surface. The calculated energetics of adsorbate structures provides arguments for the possibility of a coverage-driven phase transition from a rectangular to oblique surface structure.

ACKNOWLEDGMENTS

We are grateful to the Center for Scientific Computing (CSC), Espoo, Finland, for generous allocation of computer resources. A.K. acknowledges with thanks the hospitality of the Laboratory of Physics of HUT during his on leave stay in Helsinki. This research has been supported by the Academy of Finland through the Centers of Excellence Program (2000-2005).

[1] O.M. Braun and V.K. Medvedev, Usp. Fiz. Nauk **157**, 631 (1989) [Sov. Phys. Usp. **32**, 328 (1989)].
[2] T.L. Einstein, in *Handbook of Surface Science*, edited by W.N. Unertl (Elsevier Science, Amsterdam, 1996), Vol. 1, Chap. 11.
[3] I. Lyuksyutov, A.G. Naumovets, and V. Pokrovsky, *Two-Dimensional Crystals* (Academic Press, New York, 1992).
[4] M.S. Gupalo, V.K. Medvedev, B.M. Palyukh, and T.P. Smereka, Sov. Phys. Solid State **21**, 568 (1979).
[5] D. Kolthoff and H. Pfnür, Surf. Sci. **457**, 134 (2000).
[6] D. Kolthoff and H. Pfnür, Surf. Sci. **459**, 265 (2000).
[7] A. Fedorus, D. Kolthoff, V. Koval, I. Lyuksyutov, A.G. Naumovets, and H. Pfnür, Phys. Rev. B **62**, 2852 (2000).
[8] A. Fedorus, G. Godzik, V. Koval, A. Naumovets, and H. Pfnür, Surf. Sci. **460**, 229 (2000).
[9] G.A. Katrich, V.V. Klimov, and I.N. Yakovkin, J. Electron Spectrosc. Relat. Phenom. **389**, 48 (1997).
[10] J. Neugebauer and M. Scheffler, Phys. Rev. B **46**, 16 067 (1992).
[11] B. Gumhalter and W. Brenig, Surf. Sci. **336**, 326 (1995).
[12] F. Bagehorn, J. Lorenc, and Cz. Oleksy, Surf. Sci. **349**, 165 (1996).
[13] P. Hohenberg and W. Kohn, Phys. Rev. **136**, B864 (1964).
[14] W. Kohn and L.J. Sham, Phys. Rev. **140**, A1133 (1965).
[15] J.P. Perdew, J.A. Chevary, S.H. Vosko, K.A. Jackson, M.R. Pederson, D.J. Singh, and C. Fiolhais, Phys. Rev. B **46**, 6671 (1992); **48**, 4978(E) (1993).
[16] G. Kresse and J. Hafner, J. Phys.: Condens. Matter **6**, 8245 (1994).
[17] The Vienna *ab initio* simulation package (VASP) was developed at the Institut für Theoretische Physik of the Technische Universität Wien: G. Kresse and J. Hafner, Phys. Rev. B **47**, 558 (1993); **49**, 14 251 (1994); G. Kresse and J. Furthmüller, *ibid.* **54**, 11 169 (1996).
[18] H.J. Monkhorst and J.D. Pack, Phys. Rev. B **13**, 5188 (1976).
[19] M. Methfessel and A.T. Paxton, Phys. Rev. B **40**, 3616 (1989).
[20] Ch. Kittel, *Introduction to Solid State Physics*, 7th ed. (Wiley, New York, 1996).
[21] WebElements—periodic table of the elements (http://www.webelements.com/).
[22] J.G. Che, C.T. Chan, W.-E. Jian, and T.C. Leung, Phys. Rev. B **57**, 1875 (1998).
[23] D. Kolthoff, H. Pfnür, A.G. Fedorus, V. Koval, and A.G. Naumovets, Surf. Sci. **439**, 224 (1999).
[24] R. Smoluchowski, Phys. Rev. **60**, 661 (1941).
[25] M.W. Finnis and V. Heine, J. Phys. F: Met. Phys. **4**, L3 (1974).
[26] Y. Tian, K.-W. Lin, and F. Jona, Phys. Rev. B **62**, 12 844 (2000).
[27] D. Tomanek and K.H. Benneman, Surf. Sci. **163**, 503 (1985).
[28] S. Berge, P.O. Gartland, and B.J. Slagsvold, Surf. Sci. **43**, 275 (1974).
[29] R.D. Diehl and R. McGrath, J. Phys.: Condens. Matter **9**, 951 (1997).
[30] A. Kiejna and K.F. Wojciechowski, *Metal Surface Electron Physics* (Pergamon, Oxford, 1996).
[31] A.G. Naumovets, M.V. Paliy, Yu.S. Vedula, A.T. Loburets, and N.B. Senenko, Prog. Surf. Sci. **48**, 59 (1995).
[32] P. Hyldgaard and M. Persson, J. Phys.: Condens. Matter **12**, L13 (2000).
[33] I.N. Yakovkin, Surf. Sci. **389**, 48 (1997).
[34] H.-K. Jeong, T. Komesu, I.N. Yakovkin, and P.A. Dowben, Surf. Sci. **494**, L773 (2001).
[35] K.H. Lau and W. Kohn, Surf. Sci. **65**, 607 (1977).
[36] S. Ovesson, A. Bogicevic, G. Wahnström, and B.I. Lundqvist, Phys. Rev. B **64**, 125423 (2001).